Journal of Operation and Automation in Power Engineering

Vol. XX, No. XX, Dec. 2022, Pages: XXXX (Proofed)

http://joape.uma.ac.ir

Research Paper

Energy Efficiency and Emission Reduction through Smart Demand Side Management with Hybrid Renewable Integration Using Modified Coati Optimization Algorithm

Sampatirao Nanibabu , *Shakila Baskaran* , and *Prakash Marimuthu* *

Department of Electrical and Electronics Engineering, National Institute of Technology Nagaland, Dimapur, 797103, Nagaland, India.

Abstract— *Excessive reliance on conventional energy sources and inadequate load management strategies have triggered severe climatic impacts and created an imbalance between energy supply and demand. To address this issue, integrating smart, controllable devices with renewable energy sources and battery energy storage systems within the distribution grid enables consumers to participate actively in demand-side management strategies. Demand-side management enhances demand flexibility, reduces energy procurement costs, minimizes peak load fluctuations, and decreases emissions. This study introduces a novel demand-side management framework that includes a life cycle analysis of hybrid renewable energy systems optimized using the Modified Coati Optimization Algorithm. A hybrid renewable energy system comprising solar photovoltaic panels, wind turbines, and battery energy storage systems is deployed across the residential, commercial, and industrial sectors to assess the impact of demand-side management on cost savings, peak demand reduction, and emissions mitigation. The proposed optimization method is compared with Particle Swarm Optimization, Grey Wolf Optimization, and the standard Coati Optimization Algorithm. The results indicate that the Modified Coati Optimization Algorithm achieves cost savings of 31.45%, 31.89%, and 28.21% in the residential, commercial, and industrial sectors, respectively. Peak load reductions of 37.64%, 29.37%, and 25.63% are also achieved. Significant emission reductions are documented as totaling 3,743.11 kilograms of carbon dioxide, 28.37 kilograms of sulfur dioxide, and 17.25 kilograms of nitrogen oxides. The improved convergence of the Modified Coati Optimization Algorithm strengthens the implementation of demand-side management, making it a vital tool for optimizing energy management in smart grids.*

Keywords—Demand side management, smart grid, renewable energy sources, battery energy storage system, coati optimization algorithm.

1. Introduction

The conventional electrical grid, which forms the foundation of our contemporary civilization, has served us well for over a century. However, a revolutionary transition is underway due to the complex problems being faced in the areas of energy sustainability, reliability, and efficiency. "Smart Grid" (SG): a dynamic and self-healing power network for sustainable energy production, utilizing innovative technology to usher in a new era of energy management [1]. The electrical grid is combined with modern computers, data analytics, and automation to perform the roles in SG. This upgrade enables real-time monitoring, optimization, and responsiveness to shift energy demands and handle critical circumstances. The contemporary grid contrasts with the conventional grid, which primarily transports electricity from power plants to customers with two-way communication. This intelligent infrastructure paves the way for a more robust and environmentally friendly energy ecosystem by facilitating improved management of energy resources, incorporating renewable energy sources, and utilizing Demand-Side Management (DSM) measures [2]. A confluence of factors drives this transition. Integrating electric vehicles and deploying renewable energy sources like solar and wind are required to minimize greenhouse gas emissions. With several advantages, including increased reliability, higher energy efficiency, lower operating costs, and resilience against interruptions, the SG is considered the best choice for a step toward sustainability [3]. DSM is a concept that initially emerged in the late 1970s to address the rising cost of electricity [4]. In general, DSM entails the planning, execution, and supervision of all actions intended to affect consumers' power consumption patterns to affect the load curve beneficially [5]. DSM focuses on modifying the consumer load profile to deliver energy consumption in the most viable way. It makes use of load management techniques such as peak clipping [6], valley filling [7], load shifting [8], strategic conservation [9], strategic load growth [10], and flexible load shape [11] to control load curves in numerous ways. The peak clipping technique uses a direct control method to limit consumers' power consumption. The valley filling technique reduces the Peak Average Ratio (PAR) to aid the generation plants to work more efficiently by loading near their maximum capacity. The load-shifting technique uses the combined peak-clipping and valley-filling techniques. Some of the loads in peak load hours will be disconnected and connected in off-peak hours so that the peak load and PAR will be reduced simultaneously. The strategic conservation method reduces the overall load by using the energy efficiency method by replacing power-hungry appliances with highly efficient low-power appliances. Increasing market load share results in an overall rise in electricity sales using the strategic

Received: 24 Oct. 2024
Revised: 07 Apr. 2025
Accepted: 09 Apr. 2025
*Corresponding author:
E-mail: prakash@nitnagaland.ac.in (P. Marimuthu)
DOI: 10.22098/joape.2025.16074.2242

load growth strategy. The foundational principle of the flexible load-shape approach is the creation of contracts between utilities and participants in consumer programs to allow the latter to adjust their power consumption in exchange for financial incentives, as needed. Compared to other DSM strategies, load shifting offers a promising option that offers maximum flexibility and value to end customers and reliable income for the utility.

Modern power systems face challenges, especially in developing countries, due to rapid load growth and renewable energy integration. Extreme weather events can cause voltage drops and blackouts, highlighting the need for demand response programs (DRPs) to enhance grid stability. Studies show that implementing DSM strategies in Iran's industrial and commercial sectors led to significant demand reductions, improving economic and environmental sustainability [12]. The transition from fossil fuels to renewable energy in electric power systems necessitates efficient and reliable management in the face of load uncertainties. A probabilistic demand-side management (DSM) framework utilizing a modified artificial bee colony (MABC) algorithm demonstrated a 25.47% improvement in saving utility costs (SUC) on a modified IEEE RTS-79 system under varying peak demands [13]. A tri-objective optimization model combining demand response, real-time pricing, and network reconfiguration enhances distribution network performance, achieving up to 31% peak shaving and 80% reliability improvement using hybrid optimization methods [14]. DSM also enhances techno-economic performance in Karnataka's hybrid renewable energy systems (HRES), decreasing net present cost by 33% and energy cost by \$0.003/kWh, with lithium-ion batteries under Combined Dispatch proving optimal [15]. Short-term microgrid optimization using the Grey Wolf Optimizer has showcased significant reductions in operational costs and emissions through DSM [16]. In Renewable Energy Communities, demand-side management (DSM) implemented via genetic algorithms has improved performance and user benefits [17], while demand-side management based on the Butterfly Optimization Algorithm in commercial areas has achieved an 18.4% cost reduction and a 17.68% peak load reduction [18]. These strategies ensure a more stable, cost-effective, and sustainable energy system. Increasing energy consumption during peak hours leads to higher losses and increased environmental pollution. Demand-Side Management (DSM) programs mitigate this through load-shifting techniques. An Improved Sine Cosine Algorithm (ISCA) for energy optimization in Smart Urban Buildings (SUBs) effectively reduces electricity costs, emissions, and the peak-to-average ratio compared to the Grasshopper Optimization Algorithm (GOA), ensuring energy efficiency and user comfort [19].

Smart grids enable the integration of renewable energy (RE) sources and the management of smart appliances. Since RE sources such as geothermal, biomass, and biogas are widely available and environmentally beneficial, RE-based power generation offers significant advantages [20]. However, integrating RE into power systems presents two major challenges. The stochastic and intermittent nature of non-dispatchable RE can cause grid instability. Additionally, as RE penetration increases, conventional power systems face difficulties adapting to fluctuating generation patterns [21]. Hybrid renewable energy systems (HRES) combine multiple RE sources to enhance reliability and mitigate intermittency issues. The most common HRES configuration includes solar and wind due to their complementary nature. A backup generator or grid connection is often required to ensure system stability. Battery energy storage systems (BESS) enhance RE utilization by storing excess energy and supplying it when needed. BESS is widely used for reliability enhancement, transmission upgrades, and energy management [22]. Despite their technological reliability, further cost reductions are necessary for broader adoption [23]. Energy communities promote sustainable energy by engaging consumers; however, pilot projects often face challenges due to unpredictable consumer behaviors. Residential load datasets and surveys offer insights for DSM implementation. A genetic algorithm-based optimization reduces peak load by 29% and achieves a 9% energy bill saving, though current dataset limitations hinder further DSM efficiency [24].

In numerous studies, multiple indicators are employed to evaluate the functionality of the DSM. The typically utilized indices include the load factor (LF), peak-to-average ratio (PAR), and total cost. The ratio of peak load to average load during a given period, usually in a day, a week, a month, etc., is known as PAR. The total cost is computed by multiplying the hourly load by the hourly electricity price. The ratio of the average electricity demand to the peak load for a specific time is known as the load factor. When a DSM application is applied successfully in a system, the system's PAR is decreased, which lowers the overall cost of electricity.

Several research are ongoing in applying DSM in smart grids by integrating renewable energy sources. The prime objectives of this research are to reduce the operation cost and the system's peak load. Rehmat *et al.* have developed a hybrid standalone renewable-battery system for a household to apply DSM. The authors have optimized three configurations using solar PV, WT, and Battery Energy Storage (BES) systems (PV-BES, WT-BES, and PV-WT-BES) using fuzzy logic. The findings indicate that using DSM can lower system costs and the quantity of battery storage needed [25]. Kalim *et al.* adopted the DSM strategy for the day ahead smart grid scheduling using distributed energy resources. The authors have considered four case studies for solving three objectives in different combinations to check the better combination for the implementation of DSM using the multi-objective genetic algorithm method. The results reveal that the case study performs better in reducing the costs and emissions [26].

A home energy management control system was created by Nadeem *et al.* to implement DSM by incorporating RE sources. The authors also implemented genetic algorithms, binary PSO, and wind-driven optimization (WDO) to compare with the suggested hybrid genetic wind-driven optimization. The findings demonstrate that the suggested methodology reduces energy costs by up to 48% and the peak-to-average ratio by up to 37.69% [27]. Yadav *et al.* applied DSM in a smart distribution grid consisting of residential, commercial, and industrial areas integrated with solar PV by using the Grey Wolf Optimization (GWO) algorithm to reduce the cost of electricity and peak load in all three areas. The results show that with the help of renewable energy integration, more reductions have been achieved in the cost and peak load [28]. To determine the optimal size of a hybrid solar and wind-based renewable energy system, Geleta *et al.* have implemented the GWO algorithm. the GWO algorithm results have been compared with PSO and other related research to check the feasibility. Results show that the GWO algorithm has shown better performance [29]. To tackle rising electricity costs from demand-supply gaps, a hybrid Ant Colony Optimization (ACO) and Genetic Algorithm is proposed. It overcomes ACO's convergence issues, reducing peak load by 35.4% and achieving a 33.67% cost saving compared to unscheduled and traditional ACO methods, offering a more sustainable energy management approach [30].

Almehizia *et al.* have implemented DSM by using an enhanced genetic algorithm technique to minimize the impact of intermittency by replacing the value storage method with a large-scale BES system. The results show a significant reduction in the cost of operation in the industrial areas [31]. Ali *et al.* have adopted the day-ahead load scheduling problem by using the DSM strategy to reduce operational cost, load curtailment cost, pollution emission, and coordination between shiftable loads and wind turbines' output power. This multi-objective problem has been solved by using the multi-objective WDO technique to obtain the best solution. The results show that the proposed method efficiently achieves all the objectives [32].

Despite extensive research on Demand Side Management (DSM) in smart grids that incorporate Renewable Energy (RE) sources, several critical challenges remain unaddressed. One major issue is managing the uncertainties associated with RE sources. The stochastic and intermittent nature of solar and wind energy leads to fluctuations in power generation, which causes instability in the power grid. Although various optimization techniques have been utilized to mitigate these uncertainties, there is still a lack of models that explicitly optimize DSM while accounting for real-time RE variability. Another challenge is the need for a novel optimization algorithm. Traditional methods, such as Particle Swarm Optimization (PSO), Grey Wolf Optimization (GWO), and Genetic Algorithms (GA), often experience premature convergence and result in suboptimal solutions. These limitations underscore the need for an advanced optimization method that improves convergence speed, solution accuracy, and overall DSM performance. Additionally, the implementation of DSM across multiple load sectors remains underexplored. Most studies focus on residential, commercial, or industrial load areas in isolation, lacking a comprehensive strategy that integrates all three sectors to achieve optimal cost savings and reduce peak demand. To bridge these gaps, this study proposes a Modified Coati Optimization Algorithm (mCOA) for implementing DSM in the residential, commercial, and industrial sectors, integrating hybrid RE systems with Battery Energy Storage Systems (BESS). The proposed framework effectively enhances cost savings, reduces peak load, and minimizes emissions while demonstrating superior performance compared to conventional optimization methods.

Key contributions of the article:

- A comprehensive DSM framework is proposed that integrates Renewable Energy (RE) sources, Battery Energy Storage Systems (BESS), and smart controllable devices to optimize costs, peak demand, and emissions in residential, commercial, and industrial sectors.
- The proposed approach includes life cycle analysis of integrated photovoltaic (PV) and wind turbine (WT) systems, evaluating their economic and environmental effects on grid operations.
- This study presents a novel modified Coati Optimization Algorithm (mCOA) specifically designed for Demand-Side Management (DSM) applications. Compared to traditional algorithms, this algorithm enhances convergence speed and optimization accuracy.
- The proposed methodology greatly decreases energy procurement costs and greenhouse gas emissions, fostering a more sustainable and efficient smart grid infrastructure.

2. PROBLEM FORMULATION

The load scheduling DSM technique adopted by the Control Centre (CC) arranges shiftable device connection instances so that the load curve is near the objective demand curve. The distribution utility is assumed as CC and is responsible for carrying the load-shifting operations with the inclusion of controllable devices. The load scheduling method can be mathematically represented as minimization problem and is given below in Eq. (1) [28].

$$\text{Minimise} \sum_{t=1}^{T} (P_{act}(t) - P_T(t))^2 \tag{1}$$

Here, $P_T(t)$ is the instantaneous power of the target load, and $P_{act}(t)$ is the actual consumption of power at time t.

The following Eq. (2) is used to evaluate $P_{act}(t)$.

$$\begin{aligned} P_{\text{act}}(t) = P_L(t) + \text{Connected}(t) - \text{Disconnected}(t) - \\ P_{\text{pv}}(t) - P_{\text{wt}}(t) - P_{\text{bat}}(t) \end{aligned} \tag{2}$$

$P_L(t)$ is the power consumption of load at time t before applying DSM. The amount of load connected at time t from the controllable devices is denoted as Connected (t). From the present time 't,' some controllable loads are scheduled to be disconnected during the load-shifting process and are represented as Disconnected (t). $P_{pv}(t)$ is the solar power generated at time t, $P_{wt}(t)$ is the wind power generated at time t, and $P_{bat}(t)$ is the power from the battery energy storage system.

$P_{pv}(t)$, and $P_{wt}(t)$ are calculated mathematically by using the Eqs. (3) and (4) below.

$$P_{\text{pv}}(t) = \eta_{\text{pv}} \times A_C \times H_{(\text{pu})} \tag{3}$$

$$P_{\text{wt}}(t) = 0.5 \left(\eta_w \times \rho_{\text{air}} \times C_p \times A \times V^3 \right) \tag{4}$$

Where, η_{pv} is the efficiency of the PV array, and the total area covered by the solar array is denoted by A_C in m^2, $H_{(pu)})$ is solar irradiance in kWh/m^2, η_w is the efficiency of the WT, ρ_{air} is the density of air, based on geometric characteristics, the power factor of WT is denoted as C_p, A is the total circumference area covered by the wind turbine blades when in rotation [28]. The power of solar PV array output depends on weather conditions and temperature. In this article, the weakest operation of a PV array has been considered to recreate real-time energy harvesting from solar power.

For effective utilization of renewable energy, the available power from renewable sources must always be less than or equal to the total load demand. This balance is maintained by optimizing the battery's charging and discharging patterns, as formulated in Eq. (5).

$$P_{\text{pv}}(t) + P_{\text{wt}}(t) \leq P_{\text{act}}(t) - P_{\text{bat}}(t) \tag{5}$$

During DSM implementation, the battery's charging and discharging processes are regulated and optimized to maximize cost savings. The battery's State of Charge (SoC) is continuously updated using Eq. (6) throughout this process. Additionally, the charging and discharging power is controlled within predefined limits, as specified in Eqs. (7), (8), and (9).

$$\begin{aligned} \text{SoC}^B(t) = \text{SoC}^B(t-1) + \\ \text{SoC}^B_{\text{ch}}(t-1) - \text{SoC}^B_{\text{dis}}(t-1) \end{aligned} \tag{6}$$

$$\text{SoC}^B_{\text{ch}}(t-1) = 1 - \frac{E^B_{\text{max}} - \left(\frac{E^B_{\text{max}}}{P^B_{\text{ch}}(t)} \right)}{E^B_{\text{max}}} \tag{7}$$

$$\text{SoC}^B_{\text{dis}}(t-1) = 1 - \frac{E^B_{\text{max}} - \left(\frac{E^B_{\text{max}}}{P^{EV}_{\text{dis}}(t)} \right)}{E^B_{\text{max}}} \tag{8}$$

$$\text{SoC}^B_{\text{min}} \leq \text{SoC}^B \leq \text{SoC}^B_{\text{max}} \tag{9}$$

Here, $SoC^B(t)$ represents the available State of Charge (SoC) of the battery during DSM operation, while $SoC^B(t-1)$ denotes the available SoC from the previous hour, SoC^B_{ch} and SoC^B_{dis} indicate the SoC status of the battery during charging and discharging, respectively. E^B_{max} refers to the maximum energy capacity of the battery. Additionally, $P^B_{ch}(t)$ and $P^{EV}_{dis}(t)$ represent the battery's charging and discharging power at time t.

The Connected (t) is divided into two different components, the first component is the growth in demand at time t that have been relocated to that time, and the second component is the increment in demand at time t that were connected before time t and are still operating at time t. The Connected (t) can be calculated using the Eq. (10) given below.

$$\text{Connected}(t) = \sum_{x=1}^{t-1}\sum_{k=1}^{D}(C_{kxt}P_{1k}) + \sum_{a=1}^{j-1}\sum_{x=1}^{t-1}\sum_{k=1}^{D}\left(C_{kx(t-1)}P_{(1+a)k}\right) \quad (10)$$

Where,

x = The time from where the load got disconnected to get connected at time t.

C_{kxt} = Integer denoting the number of type k devices whose operating time got shifted from x to t

k = Type of the device

D = The total number device types

P_{1k} = Power consumption of k type devices during first hour of operation

$P(1+a)k$ = Power consumption of k type devices during later hours of operation

j = The k-type devices' overall energy consumption time

Similarly, there are two components in Disconnected (t): The reduction in demand brought by the delay in the operating schedule of devices that were previously planned to operate and continue working in the present time and the reduction in load brought by the delay in the operating schedule of devices that were originally planned to operate at time step t. the Disconnected (t) is given by the following Eq. (11).

$$\text{Disconnected}(t) = \sum_{b=t+1}^{t+q}\sum_{k=1}^{D}(C_{ktb}P_{1k}) + \sum_{a=1}^{j-1}\sum_{b=t+1}^{t+q}\sum_{k=1}^{D}\left(C_{k(t-1)b}P_{(1+a)k}\right) \quad (11)$$

Where, C_{ktb} is the number of type k devices that will delay from time t to time b in the future, and q is the maximum allowable delay in any type of device based on the consumer's satisfaction level.

The prime objective of the load scheduling DSM strategy is to reduce the total electricity price. The objective function has been formulated such that the load power is inversely proportional to the price of electricity during that period. Mathematically represented as given in Eq. (12).

$$\text{Objective}(t) = \left(\frac{\text{Averageprice}}{\text{Maximumprice}} \times \sum_{t=1}^{T=24}\text{Forecasted}(t)\right) \times \frac{1}{\text{Price}(t)} \quad (12)$$

The objective function of load scheduling DSM is bound to the following constraints as given in Eqs. (13) to Eq. (15). The number of devices that can be controlled from any hour cannot be negative. There should always be a greater number of shiftable devices at a given instant than the number of devices that are shifting from that instant.

$$C_{kxt} > 0, \quad \forall x,k,t \quad (13)$$

$$\sum_{t=1}^{T} C_{kxt} \leq \text{Controllable}(x) \quad (14)$$

Where, Controllable (x) is the quantity of controllable devices at time x. The time allotment for any controllable load can only be postponed but never be preponed. This can be expressed numerically as,

$$C_{kxt} = 0, \quad \forall x > t \quad (15)$$

When applying DSM by managing any type of load, customers should not experience inconvenience due to delays in the device's operating time. During load shifting, devices that fall under the curtailed load will turn off for a certain duration. Longer curtailments lead to greater inconvenience for customers. This article assumes that customers will not be inconvenienced if the maximum allowable duration for any device participating in the load-shifting program is 10 hours [33].

The emissions generated from coal-fired thermal plants are estimated as 950 grams of CO_2, 7.20 grams of SO_2, and 4.38 grams of NO for every kWh of energy produced by a coal-fired power plant. Total emission production can be calculated in any area of the smart grid by using the (16) given below [34].

$$E_{\text{Total}} = (E_{\text{CO}_2} + E_{\text{SO}_2} + E_{\text{NO}})\sum_{t=1}^{24} P_{\text{act}}(t) \quad (16)$$

Where The total emission for the whole day is represented by E_{Total}, E_{SO_2}, E_{SO_2}, and E_{NO} are denoted as the amount of CO_2, SO_2, and NO generated for each kWh of energy produced respectively in grams.

Hourly forecasted load demand data for residential, commercial, and industrial areas has been shown in Fig. 1. The graph has plotted a complete 24-hour load through which peak load and peak-to-average ratio have been calculated as follows. The peak load of 1363.6 kW, 1818.2 kW, and 2678 kW were recorded in residential, commercial, and industrial areas. The peak-to-average ratio is calculated as the ratio of peak load to the average load recorded during the day, which has given 1.852, 1.7, and 1.607, respectively, in all the areas.

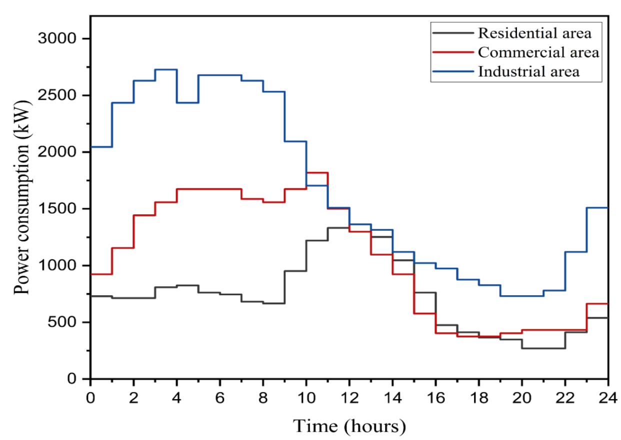

Fig. 1. Hourly load data in residential, commercial, and industrial areas.

2.1. Design variables for solar PV, wind, and battery hybrid system

Table 1 represents the battery, solar PV, and WT generator design variables. From this table, the cost of energy per unit has been calculated as 3.33 rupees, 4.352 rupees, and 10.137 rupees for solar PV, WT, and BESS, respectively. All values have been calculated by assuming that all the resources are working at their 50% capacity.

Solar data was computed using the Photovoltaic Geographic Information Sector (PVGIS), which offers free access to solar data for every location on Earth. The installed PV plant's capacity in the smart grid is considered 200kW. The hourly forecasted photovoltaic power and wind power data are shown in Table 2 [35].

Table 1. Design variables of hybrid energy system [35].

	Parameters	Values	unit
Battery	Span of life	5	Years
	Round trip efficiency	80	%
	Installation cost	200	Indian Rupees/kWh
	O&M cost	500	Indian Rupees/kWh/year
	Depth of Discharge	60	%
	Capacity	200,500,800	kWh
PV array	Span of life	20	Years
	Efficiency	16	%
	Installation cost	1000	Indian Rupees/kW
	O&M cost	15	Indian Rupees/kW/year
Wind turbine generator	Span of life	20	Years
	Cut-in/ Cut-off/ Rated speed	3/ 25/ 9.5	m/s
	Investment cost	1300	Indian Rupees/kW
	O&M cost	30.33	Indian Rupees/kW/year
	Hub height	60	Meters

Table 2. Solar PV and wind power prediction data.

Time (Hours)	Solar power (kW)	Wind power (kW)	Time (Hours)	Solar power (kW)	Wind power (kW)
8	127	109.94	20	0	106.36
9	157.5	112.59	21	0	97.78
10	175.83	108.01	22	0	95.17
11	183.83	113.86	23	0	91.075
12	178.91	123.18	24	0	96.02
13	162.33	119.43	1	0	99.77
14	136.75	113.92	2	0	93.6
15	97.83	117.44	3	0	92.325
16	50.33	119.2	4	0	99.315
17	10.41	110.055	5	2	105
18	0	111.42	6	3.25	110.325
19	0	111.93	7	83.83	112.61

3. Modified Coati Optimization Algorithm (MCOA)

Optimization techniques are crucial in various fields, including finance, engineering, logistics, and healthcare. Their primary aim is to identify the most effective solution to a problem, whether through efficiency improvement, cost reduction, or achieving other desirable outcomes. In complex systems where multiple factors interact, it is often impractical or impossible to explore every possible solution manually. Optimization algorithms automate this process, systematically searching the solution space to identify the best configuration. By utilizing mathematical algorithms, optimization strategies enhance informed decision-making, optimize resource allocation, and improve overall performance.

Optimization algorithms, such as Particle Swarm Optimization (PSO) and the Coati Optimization Algorithm (COA), have proven effective in solving complex problems, including energy management and demand-side management (DSM). However, they face limitations in terms of convergence speed, solution accuracy, and the exploration-exploitation balance when applied to large-scale, dynamic DSM scenarios. PSO and COA often experience stagnation in later optimization stages due to inadequate adaptive mechanisms, leading to increased computational time and inefficient real-time decision-making. Additionally, their solution accuracy declines in high-dimensional search spaces, with PSO suffering from premature convergence and COA struggling to escape local optima. These challenges reduce their effectiveness in managing load demands and integrating renewable energy. Furthermore, their inability to maintain an optimal balance between exploration and exploitation limits their adaptability to sudden changes in the grid. This results in suboptimal energy dispatch, higher operational costs, and poor utilization of renewable resources. To overcome these challenges, modifying the Coati Optimization Algorithm is essential. The proposed enhancements introduce adaptive strategies to improve convergence speed, refine the exploration-exploitation mechanism, and enhance solution accuracy. The modified algorithm ensures efficient load management, cost reduction, and improved system stability. These improvements contribute to the development of sustainable and resilient energy management systems, supporting the integration of renewable energy and advancing modern smart grid operations.

PSO is inspired by the social behavior of birds flocking or fish schooling. PSO searches the search space for the best possible solution by moving a population of viable solutions, referred to as particles, through it. Each particle adjusts its position based on its personal best-known position and the global best-known position found by any particle in the swarm. Through iterations, particles converge towards the optimal best solution [36].

Coatis, often known as coatimundis, are Procyonidae (Nasua and Nasuella) family members. A green iguana is one of the coatis' favourite foods. In general, Iguanas are large reptiles that usually lives in trees and the coatis are considered to get divided into two groups for hunting. The first group of coatis are assumed to climb the tree, for scaring the iguana and to make it jump off the tree. The successive group attacks the fallen iguana swiftly. However, coatis themselves are susceptible to predator attacks. Jaguars, tayras, dogs, foxes, ocelots, maned wolfs, anacondas etc. are few such predators. The COA technique was developed based on coati's predating tactics against iguanas and their behaviour of escaping when confronting with predators [37].

According to the COA technique, coatis are considered as group of members., which is classified as a population-based metaheuristic algorithm. The values for the variables are determined based on each coati's position in the predefined search space. At the beginning of the COA implementation, the position of each coati is randomly initialized in the search space using the Eq. (17) given below.

$$X_i : x_{i,j} = \mathrm{lb}_j + r(\mathrm{ub}_j - \mathrm{lb}_j),\\ i = 1, 2, \ldots, N, \text{ and}\\ j = 1, 2, \ldots, m \tag{17}$$

where X_i is the i^{th} coati's location, $x_{i,j}$ is the value of the j^{th} variable, population of coatis represented with N, r is initialized randomly in the interval [0, 1], m is the number of variables, and lb_j, ub_j are the lower and upper bound of the j^{th} variable, respectively.

By using the matrix given in Eq. (18), the population of coatis In the COA are mathematically represented as,

$$X = \begin{bmatrix} X_1 \\ \vdots \\ X_i \\ \vdots \\ X_N \end{bmatrix}_{N\times 1} = \begin{bmatrix} x_{1,1} & \cdots & x_{1,j} & \cdots & x_{1,m} \\ \vdots & \ddots & \vdots & \ddots & \vdots \\ x_{i,1} & \cdots & x_{i,j} & \cdots & x_{i,m} \\ \vdots & \ddots & \vdots & \ddots & \vdots \\ x_{N,1} & \cdots & x_{N,j} & \cdots & x_{N,m} \end{bmatrix}_{N\times m} \tag{18}$$

Any one of two coati natural behaviours is used to update the location of coatis in the COA. These actions consist of:

1) The strategy used by coatis to attack iguanas,
2) The strategy of coati while it is escaping from a predator.

The strategy of coati while hunting the iguana comprises of different steps. A group of coatis divided equally into two groups, in which first group of coatis climb the tree to scare the iguana, and the second group of coatis wait under the tree to attach iguana when it falls from the tree. In this strategy of implementation, the location of iguana is assumed by the position of best coati in the group. The position of the coatis climbing the tree is represented using Eq. (19).

$$X_i^{P1} : x_{(i,j)}^{P1} = x_{(i,j)} + r \cdot (\text{Iguana}_j - x_{(i,j)}), \\ \text{for} i = 1, 2, \dots, \left[\frac{N}{2}\right], \; and \; j = 1, 2, \dots, m. \tag{19}$$

The standard Coati Optimization Algorithm (CoA) updates coati positions using a random mechanism, enhancing exploration. However, this randomness often causes the algorithm to get trapped in local minima or converge prematurely, reducing its efficiency in large-scale optimization problems like demand-side management. To overcome this, a modified Coati Optimization Algorithm (mCOA) is proposed, incorporating a coefficient that simulates the predator's encircling mechanism. This adaptation improves the balance between exploration and exploitation, preventing early convergence and enhancing solution accuracy. The dynamic adjustment of the coefficient further ensures faster convergence and greater stability. The mathematical expression for this modification is presented in Eq. (20). The coefficient introduced in the mCOA ensures that the search agents dynamically adjust their movements based on the best-known solution, encouraging more strategic exploration in the search space. This prevents excessive randomness, leading to improved solution accuracy. Additionally, the encircling mechanism promotes a gradual convergence toward the global optimum by keeping search agents within an adaptive boundary.

$$X_i^{P1} : x_{(i,j)}^{P1} = x_{(i,j)} + \vec{A} \cdot (\text{Iguana}_j - x_{(i,j)}), \\ \text{for} i = 1, 2, \dots, \left[\frac{N}{2}\right], \; and \; j = 1, 2, \dots, m. \tag{20}$$

After the iguana falls from the tree, the position of it can be placed by generating a position randomly in search space, which is represented mathematically using Eq. (21).

$$\text{iguana}^c : \text{iguana}_j^c = ib_j + r \cdot (ub_j - lb_j), \\ j = 1, 2, \dots, m. \tag{21}$$

If the updated position of the coati is better than the initial location, it is acceptable; otherwise, the initial position must be given to the coati's new position. Eq. (22) can be used to depict this occurrence.

$$X_i = \begin{cases} X_i^{P1}, & F_i^{P1} < F_i, \\ X_i, & \text{else}. \end{cases} \tag{22}$$

Where, X_i^{P1} is the new updated position for i^{th} coati based on attacking phase, $X_{i,j}^{P1}$ is the position i^{th} coati at j^{th} dimension, $\vec{A} = 2\vec{a}r$ is a coefficient vector, $\vec{a}$ is a vector which drops linearly from 2 to 0, r is a random number. F_i^{P1} is the objective function value, iguana's position is represented with $iguana^c$.

Another strategy of the process of updating the position of coatis is based on, when a predator attacks a coati, it moves in a way which keeps coati being in a harmless position close to its present position. To simulate this behaviour, Eqs. (23) and (24) are used to obtain a random place close to where each coati is positioned.

$$\text{lb}_j^{\text{local}} = \frac{\text{lb}_j}{t}, \quad \text{ub}_j^{\text{local}} = \frac{\text{ub}_j}{t}, \\ \text{where} t = 1, 2, \dots, T \tag{23}$$

$$X_i^{P2} : x_{i,j}^{P2} = \\ x_{i,j} + (1 - 2r) \cdot (ib_j^{\text{local}} + r \cdot (\text{ub}_j^{\text{local}} - \text{lb}_j^{\text{local}})), \\ i = 1, 2, \dots, N, \; j = 1, 2, \dots, m \tag{24}$$

The updated position of the coati is acceptable if it is better than the initial position; otherwise, the initial position must be attributed to the coati's new location. This phenomenon has been represented by using Eq. (25).

$$X_i = \begin{cases} X_i^{P2}, & F_i^{P2} < F_i, \\ X_i, & \text{else}. \end{cases} \tag{25}$$

Where, X_i^{P2} is the new updated position for i^{th} coati based on escaping phase, F_i^{P2} is the objective function value of i^{th} coati. The complete process of working of mCOA algorithm has shown in Fig. 2.

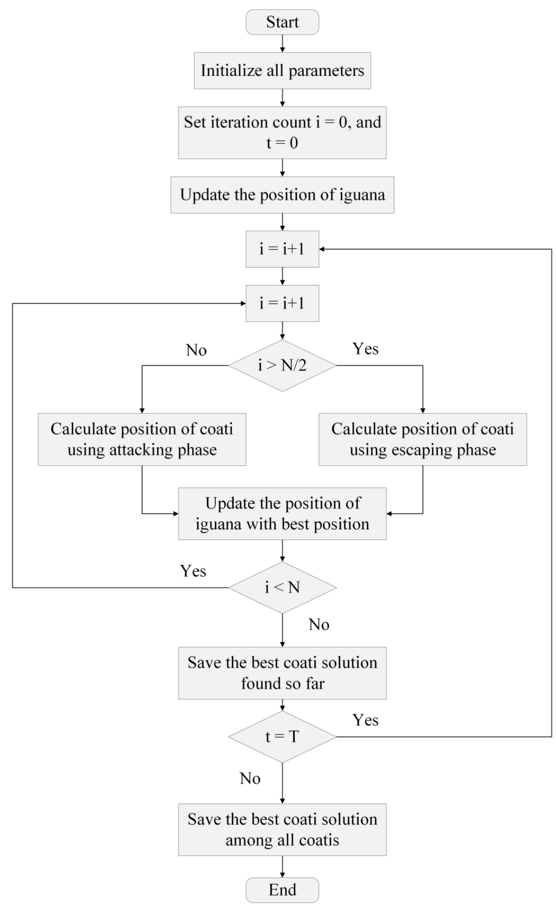

Fig. 2. Flowchart for mCOA optimization.

To validate the mCOA proposed in this article, a diverse set of benchmark functions amounting to 30 has been collected [38], and the optimal values are evaluated along with its best, median, worst, mean, and SD values as shown in Table 3 below. The simulation results show that the proposed algorithm performs better for the functions of the sphere, Beale, cigar, step, bohachevsky, rosenbrock, etc. The implemented DSM objective is similar to the power sum benchmark function, where the proposed optimization algorithm has achieved a better optimal point than another optimization algorithm, as shown in Table 4.

Table 3. Simulation results of benchmark functions.

Function	Mean	SD	Best	Median	Worst
f_1	0	0	0	0	0
f_2	0	0	0	0	0
f_3	0	0	0	0	0
f_4	0	0	0	0	0
f_5	4.1807E-05	2.5301E-05	5.7895E-05	3.4287E-05	1.4872E-05
f_6	0	0.0001E+00	0	0	0.0026E+00
f_7	1.7168E-02	0.0086E-02	1.7183E-02	1.7183E-02	1.7146E-02
f_8	1.8347E-19	2.7654E-20	1.6300E-19	1.6285E-19	2.0904E-19
f_9	3.5780E-01	2.7542E-02	2.8908E-01	2.4136E-01	4.9863E-01
f_{10}	-1.4310E+00	-1.3504E+00	-0.9701E+00	-1.0824E+00	-2.8972E+00
f_{11}	0.0078E-12	0.0015E-12	0.0000E-12	0.0063E-12	0.1260E-12
f_{12}	0.0015E-05	0.0003E-05	0.0001E-05	0.0033E-05	0.0863E-05
f_{13}	0.0009E-09	0.0003E-09	0.0000E-09	0.0001E-09	0.0026E-09
f_{14}	0.0029E-02	0.0008E-02	0.0001E-04	0.0007E-02	0.0092E-02
f_{15}	-1.0200E+00	-0.8500E+00	-1.0000E+00	-1.0080E+00	-0.0020E+00
f_{16}	-1.8196E+02	-0.0926E+02	-1.8390E+02	-1.9623E+02	-1.5863E+02
f_{17}	0	0	0	0	0
f_{18}	0.0001E-26	0.0015E-21	0	0.0001E-26	0.0001E-16
f_{19}	0.0001E-09	0.0005E-10	0	0.0001E-09	0.0006E-03
f_{20}	-4.1725E+02	-0.2158E+02	-4.1889E+02	-4.2518E+02	-4.9625E+02
f_{21}	0	0	0	0	0
f_{22}	2.8725E+00	0.5963E+00	2.9852E+00	3.1260E+00	2.6398E+00
f_{23}	0	0	0	0	0
f_{24}	0	0	0	0	0
f_{25}	0.0026E-05	0.0018E-05	0	0.0028E-05	0.0016E-06
f_{26}	-1.0024E+01	-0.5712E+01	-1.0000E+01	-1.1823E+01	-0.5639E+01
f_{27}	0	0	0	0	0
f_{28}	-1.5012E+03	-0.0216E+03	-1.5000E+03	-1.5021E+03	-1.4912E+03
f_{29}	-0.0381E+01	-0.0213E+01	-0.0379E+01	-0.0377E+01	-0.0342E+01
f_{30}	0	0	0	0	0

Table 4. Comparison of proposed mCOA with different algorithms. (BOA: Butterfly Optimization Algorithm, GA: Genetic Algorithm).

Function		mCOA	COA	BOA	GA	PSO
f_1	Mean	**0**	2.5832E-01	**0**	2.2039E-02	1.7665E-51
	SD	0	5.3190E-01	0	9.6789E-03	1.1246E-50
f_2	Mean	**0**	1.9862E-04	**0**	**0**	**0**
	SD	0	3.1284E-04	0	0	0
f_3	Mean	**0**	8.3493E-03	**0**	2.1954E-04	3.1041E-53
	SD	0	2.3470E-02	0	1.0961E-04	2.1065E-52
f_4	Mean	**0**	2.2143E-01	**0**	2.3026E-02	1.3116E-31
	SD	0	4.8828E-01	0	1.0512E-02	6.653E-31
f_5	Mean	4.1807E-05	5.0968E-01	**3.8917E-05**	2.7387E-03	3.7408E+00
	SD	2.5301E-05	1.3056E-01	2.9019E-05	8.5056E-04	1.0296E+00
f_6	Mean	**0**	**0**	**0**	**0**	3.0393E-02
	SD	0.0001E+00	0	0	0	2.6192E-17
f_7	Mean	**1.7168E-02**	3.5689E+00	1.7183E+00	4.6683E-02	1.8186E+01
	SD	0.0086E-02	6.8939E-01	0	1.6847E-02	5.4812E+00
f_8	Mean	**1.8347E-19**	5.4987E-01	1.8472E-19	5.5598E-02	4.0503E+01
	SD	2.7654E-20	2.7198E-01	2.6886E-20	2.9490E-02	4.1334E+01
f_9	Mean	3.5780E-01	3.1092E-02	4.4108E-01	**1.3732-04**	4.9297E+00
	SD	2.7542E-02	4.8193E-02	5.7467E-02	7.6553E-05	5.9951E+00
f_{10}	Mean	**-1.431E+00**	-9.426E+00	-5.338E+00	-9.660E+00	-7.75E+00
	SD	-1.350E+00	6.7972E-02	-5.609E+00	5.8796E-09	0.7118E+00
f_{11}	Mean	0.0078E-12	2.3864E+01	**0**	1.6458E+01	1.4453E+02
	SD	0.0015E-12	5.5075E+00	0	4.1090E+00	3.7957E+01
f_{12}	Mean	0.0015E-05	6.0958E+00	**0**	3.1474E-17	4.4402E-02
	SD	0.0003E-05	6.1796E-01	0	3.0784E-16	4.5318E-01
f_{13}	Mean	0.0009E-09	8.6622E-16	**0**	1.6896E-17	0
	SD	0.0003E-09	8.5387E-16	0	1.6896E-16	0
f_{14}	Mean	**0.0029E-02**	1.2571E+02	2.8837E+01	3.7872E+01	2.5746E+02
	SD	0.0008E-02	8.7373E+01	3.1281E-02	2.5254E+01	3.7311E+02
f_{15}	Mean	-1.020E+00	-9.004E-01	**-1.000E+00**	**-1.000E+00**	**-1.000E+00**
	SD	-0.850E+00	2.7310E-01	0	0	0
f_{16}	Mean	-1.819E+02	-1.860E+02	**-1.867E+02**	**-1.867E+02**	**-1.867E+02**
	SD	-0.092E+02	5.4273E-10	2.0649E-11	5.5389E-14	2.5708E-13
f_{17}	Mean	**0**	2.3648E-02	**0**	2.4244E-03	1.2030E+03
	SD	0	4.1886E-02	0	1.0716E-03	5.4485E+02
f_{18}	Mean	**0.0001E-26**	1.0006E-01	6.996E-153	4.6662E-02	1.0586E-01
	SD	0.0015E-21	6.6005E-01	1.478E-152	1.0895E-02	6.5371E-02
f_{19}	Mean	0.0001E-09	1.4218E-01	**0**	5.4367E-02	7.2800E+01
	SD	0.0005E-10	6.8338E-02	0	.6187E-02	2.2745E+01
f_{20}	Mean	-4.172E+02	-1.059E+04	-2.266E+03	-1.189E+04	-7.570E+03
	SD	-0.215E+02	2.9306E+02	4.5626E+02	2.9530E+02	8.8893E+02
f_{21}	Mean	**0**	1.3204E-11	**0**	**0**	**0**
	SD	0	2.4214E-11	0	0	0
f_{22}	Mean	2.8725E+00	**3.000E+00**	**3.0000E+00**	**3.0000E+00**	**3.0000E+00**
	SD	0.5963E+00	6.4866E-12	0	0	0
f_{23}	Mean	**0**	1.1932E-04	**0**	8.388E-104	**0**
	SD	0	1.3039E-04	0	2.516E-103	0
f_{24}	Mean	**0**	1.5105E+01	**0**	3.2713E-02	3.3671E+03
	SD	0	1.1057E+01	0	1.1145E-02	9.5201E+02
f_{25}	Mean	**0.0026E-05**	7.1343E-02	2.8400E-02	1.2997E-04	1.9839E-04
	SD	0.0018E-05	5.1375E-02	1.3179E-02	1.1326E-04	1.6590E-04
f_{26}	Mean	-1.002E+01	-1.010E+01	**-1.015E+01**	-8.900E+00	-1.150E+01
	SD	-0.571E+01	0	0	2.7008E+00	0
f_{27}	Mean	**0**	1.2211E-02	**0**	3.4256E-03	9.2000E+02
	SD	0	1.2947E-02	0	2.281E-03	8.2704E+02
f_{28}	Mean	**-1.501E+03**	3.6425E+04	-2.750E+07	-1.035E+03	7.6727E+05
	SD	-0.021E+03	1.9418E+04	5.6521E+07	1.1916E+03	4.0197E-05
f_{29}	Mean	-0.038E+01	-3.792E-03	**-3.791E-03**	**-3.791E-03**	**-3.791E-03**
	SD	-0.021E+01	5.7115E-18	0	4.5714E-19	0
f_{30}	Mean	**0**	8.0007E-03	8.0070E-03	9.565E-06	**0**
	SD	0	9.6124E-03	9.6142E-03	3.0245E-05	0

4. RESULTS AND DISCUSSIONS

The day-ahead load scheduling DSM approach has been adopted to meet the objectives of the smart distribution grid in the residential, commercial, and industrial sectors. The DSM is optimized using the modified Coati Optimization Algorithm (mCOA). With the assistance of controllable loads available in each smart distribution grid, the devices have been scheduled a day in advance to reduce the overall operational costs and peak load. The forecasted load for residential, commercial, and industrial sectors indicates peaks of 1363.3 kW, 1818.2 kW, and 2727.3 kW, respectively. To lower power consumption from the grid, each sector is equipped with 2000 kW of solar PV energy, 200 kW of wind energy, and a 200 kWh battery pack. The results obtained from the COA algorithm have been compared with those from the Particle Swarm Optimization and COA. By satisfying all constraints, the mCOA algorithm helps reduce the operational costs and peak load of the system. The results demonstrate a significant reduction in the overall operational costs and peak load of the smart grid.

The load scheduling DSM application can be implemented using various controllable loads across all areas of the smart grid. Table 5 below lists the controllable loads available in all areas of the smart grid, along with their power ratings and continuous operation durations for a day. There are a total of 2,604, 808, and 109 controllable devices in the residential, commercial, and industrial areas, respectively.

4.1. Residential area

The modified Coati Optimization Algorithm (mCOA) applied to Demand Side Management (DSM) in residential smart grids shows notable improvements in operational costs and peak load reduction. When compared to traditional algorithms such as Particle Swarm Optimization (PSO) and the standard Coati Optimization Algorithm (COA), the mCOA outperforms them by effectively optimizing energy consumption and reducing grid reliance. In scenarios lacking renewable energy (RE) integration, the mCOA achieves a 13.28% reduction in operational costs and a 29.79% decrease in peak load. When RE sources are incorporated, the savings in expenses rise to 31.35%, accompanied by a 37.64% decrease in peak load. These findings highlight the algorithm's effectiveness in managing complex, dynamic energy scenarios. The enhanced outcomes are due to the mCOA's adaptive search mechanism and its improved balance between exploration and exploitation, which help prevent premature convergence and guarantee optimal load distribution. The marked decrease in operational costs and peak load underscores the algorithm's effectiveness in facilitating the

Table 5. Hourly power consumption of controllable load devices in smart grid [28].

Type of device	Power rating (kW)	Residential area		Commercial area		Industrial area	
		Working hours	Number of devices	Working hours	Number of devices	Working hours	Number of devices
Dryer - 1	1.2	01	189	-	-	-	-
Washing machine	0.5	02	268	-	-	-	-
Iron	1	01	340	-	-	-	-
Fan	0.2	03	288	-	-	-	-
Toaster	0.9	01	48	-	-	-	-
Blender	0.3	01	66	-	-	-	-
Hair dryer	1.5	01	58	-	-	-	-
Frying pan	1.1	01	101	-	-	-	-
Dishwasher	0.7	01	288	-	-	-	-
Oven - 1	1.3	01	279	-	-	-	-
Vacuum cleaner	0.4	01	158	-	-	-	-
Kettle - 1	2	01	406	-	-	-	-
Rice cooker	0.85	01	59	-	-	-	-
Coffee maker - 1	0.8	01	56	-	-	-	-
Water dispenser	2.5	-	-	01	156	-	-
Kettle - 2	3	-	-	02	123	-	-
Coffee maker - 2	2	-	-	02	99	-	-
Air conditioner	4	-	-	03	56	-	-
Dryer - 2	3.5	-	-	01	117	-	-
Oven - 2	5	-	-	01	77	-	-
Fan/AC - 1	3.5	-	-	02	93	-	-
Lights	2	-	-	03	87	-	-
Water heater	12.5	-	-	-	-	04	39
Fan/AC - 2	30	-	-	-	-	05	16
Induction motor	100	-	-	-	-	06	5
Welding machine	25	-	-	-	-	05	35
Arc furnace	50	-	-	-	-	06	8
DC motor	150	-	-	-	-	03	6
Total	-	-	2604	-	808	-	109

integration of renewable energy resources. By lessening dependence on the primary grid, the mCOA fosters a more sustainable and resilient energy system. Moreover, its capacity to reduce peak load can alleviate pressure on grid infrastructure, boost voltage stability, and increase overall grid reliability. This holistic optimization approach establishes the mCOA as a viable and effective solution for contemporary energy management challenges.

Table 6. Cost of energy and peak load of residential smart grid after the application of DSM.

Optimization technique	Peak load (kW)		PAR		Cost (Rupees)	
	Peak load	% reduction	PAR	% reduction	cost	% reduction in cost
without DSM	1363.6	-	1.852	-	230292.4	-
[28] without RE	1039.3	23.76	1.411	23.76	212974.0	7.52
PSO without RE	1196.15	12.27	1.625	12.27	207132.6	10.05
COA without RE	1181.95	13.32	1.605	13.32	206520.7	10.32
mCOA without RE	957.32	29.79	1.301	29.79	199693.6	13.28
[28] with RE	1031.9	24.30	1.401	24.30	201390.3	12.55
PSO with RE	1087.79	20.22	1.875	-1.24	165301.1	28.22
COA with RE	1075.59	21.12	1.854	-0.008	164689.2	28.48
mCOA with RE	850.32	37.64	1.487	19.71	158075.2	31.35
PSO with RE and battery	1057.79	22.42	1.827	1.34	165514.1	28.12
COA with RE and battery	1081.52	20.68	1.867	-0.008	164902.2	28.39
mCOA with RE and battery	850.32	37.64	1.487	19.71	157862.1	31.45

The findings in Table 6 indicate that the mCOA consistently outperforms PSO and COA in both RE and non-RE situations. In scenarios involving RE integration, the mCOA achieves the highest cost savings and the largest peak load reduction, thereby optimizing the use of renewable resources and decreasing reliance on the grid. Additionally, even with a battery for energy storage, the mCOA maintains its superior performance, demonstrating its resilience in addressing dynamic energy management challenges.

Table 7 provides a detailed hour-by-hour comparison of load consumption from the power grid, indicating that the mCOA shows lower consumption levels, especially during peak hours, which helps reduce the overall peak-to-average ratio (PAR).

Table 7. Load consumption from the power grid in a residential area.

Hour	Price (Rs/kWh)	Load consumption from the power grid in residential area (kW)					
		PSO		COA		mCOA	
		Without RE	With RE	Without RE	With RE	Without RE	With RE
8	12	620.2	383.26	614.2	377.26	583.93	346.99
9	9.19	594.35	324.26	570	299.91	686.94	416.85
10	12.27	631.05	347.21	587.6	303.76	620.75	336.91
11	20.69	486	188.31	479.25	181.56	516.1	218.41
12	26.82	467.45	165.36	378.6	76.51	447.25	145.16
13	27.35	394.1	112.34	422.5	140.74	422.63	140.87
14	13.81	807.8	557.13	910.7	660.03	727.71	477.04
15	17.31	563.35	348.08	530.85	315.58	595.85	380.58
16	16.42	507.3	337.77	537.4	367.87	570.74	401.21
17	9.83	1015.65	895.18	850.9	730.43	790.74	670.27
18	8.63	1117.35	1005.93	1103.15	991.73	874.79	763.37
19	8.87	1196.15	1084.22	1147	1035.07	854.64	742.71
20	8.35	1194.15	1087.79	1181.95	1075.59	895.33	788.97
21	16.44	1092.05	994.27	1149.3	1051.52	498.5	400.72
22	16.19	877.5	782.33	891.05	795.88	502.1	406.93
23	8.87	887.3	796.22	838.65	747.57	833.79	742.71
24	8.65	720.1	624.08	790.85	694.83	857.62	761.6
1	8.11	799.4	699.63	770.1	670.33	912.09	812.32
2	8.25	752.5	658.9	747.1	653.5	892.13	798.53
3	8.1	709.8	617.47	676.25	583.92	905.94	813.61
4	8.14	585.3	485.98	638.5	539.18	898.89	799.57
5	8.13	511.8	404.8	660.65	553.65	957.32	850.32
6	8.34	549.85	436.27	595.5	481.92	917.49	803.91
7	9.35	583.8	387.36	592.25	395.81	901.03	704.59

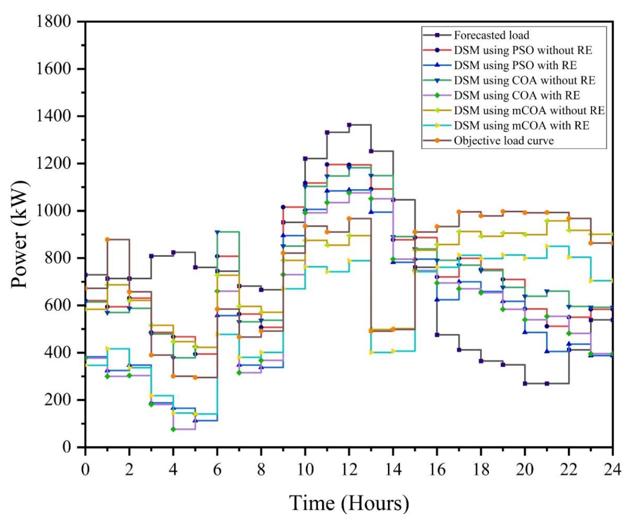

Fig. 3. Load details after applying DSM in a residential area.

The consumption pattern aligns more closely with the target load curve, as illustrated in Fig. 3. The mCOA's ability to sustain a balanced and efficient load profile enhances grid stability and lowers operational costs. In summary, the mCOA algorithm proves to be a reliable and effective optimization strategy for DSM in residential smart grids, offering significant economic and operational benefits while promoting the integration of renewable energy sources.

4.2. Commercial area

The implementation of the modified Coati Optimization Algorithm (mCOA) for Demand Side Management (DSM) in a commercial smart grid has resulted in significant reductions in operational costs and peak load demand. A comprehensive analysis indicates that mCOA outperforms other algorithms, including Particle Swarm Optimization (PSO) and the standard Coati Optimization Algorithm (COA). This advantage becomes particularly evident when renewable energy (RE) sources are integrated, improving its efficacy for cost savings and load reductions, as shown in Table 8. Without RE integration, mCOA leads to a 20.35% decline in operational costs and a 24.09% decrease in peak load. These results highlight the algorithm's effectiveness in managing energy consumption by optimizing load schedules and minimizing unnecessary expenses. The advantages of mCOA are even more pronounced with the inclusion of RE sources, where operational costs decrease by 31.89% and peak load experiences a significant reduction of 29.37%. This enhanced performance is primarily attributed to mCOA's ability to balance exploration and exploitation during optimization, which prevents premature convergence on suboptimal solutions and supports informed decision-making.

Table 8. Cost of energy and peak load of the commercial smart grid after the application of DSM.

Optimization technique	Peak load (kW)		PAR		Cost (Rupees)	
	Peak load	% reduction	PAR	% reduction	cost	% reduction in cost
without DSM	1818.2	-	1.7008	-	362664	-
[28] without RE	1438.7	20.87	1.345	20.87	328827.4	9.33
PSO without RE	1562.7	14.05	1.461	14.09	318024.6	12.30
COA without RE	1560.7	14.16	1.4599	14.16	296420.3	18.26
mCOA without RE	1380.07	24.09	1.2909	24.1	288831.1	20.35
[28] with RE	1442.7	20.65	1.349	24.30	317621.1	12.42
PSO with RE	1451.28	20.18	1.583	6.89	276193.1	23.84
COA with RE	1449.28	20.29	1.5738	7.46	254588.8	29.80
mCOA with RE	1284.05	29.37	1.419	16.56	246999.6	31.89
PSO with RE and battery	1421.28	21.83	1.553	8.69	276406.2	23.78
COA with RE and battery	1419.28	21.94	1.543	9.2	254801.8	29.74
mCOA with RE and battery	1314.05	27.72	1.452	14.62	247212.6	31.83

The hourly load consumption data in Table 9 demonstrates the effectiveness of the mCOA algorithm. Compared to PSO and COA, the mCOA consistently shows lower power consumption during peak hours, highlighting its enhanced load management efficiency. Additionally, its adaptive features ensure alignment with the target load curve, helping to maintain stable and balanced energy demand throughout the day. This performance highlights the mCOA's effectiveness in environments with fluctuating energy demands, enabling reliable and cost-effective energy management. Furthermore, the mCOA outperforms other algorithms, as indicated by the comparisons. While both COA and PSO also help reduce energy costs and peak loads, the mCOA yields superior results across all scenarios. This is particularly evident in its ability to achieve significant reductions in both expenses and load, especially within RE-integrated systems. The algorithm's alignment with the objective load curve further underscores its ability to manage load consumption patterns effectively. By minimizing sudden load surges and promoting smoother energy demand, the mCOA not only leads to cost savings but also enhances the effective use of renewable energy resources.

Using the data from Table 9, the load curve for different techniques using DSM in commercial areas has been plotted and shown in Fig. 4. The load curves show that the mCOA algorithm efficiently follows the Objective load curve when compared to all other methods.

4.3. Industrial area

The modified Coati Optimization Algorithm (mCOA) applied to Demand Side Management (DSM) in an industrial smart grid

Table 9. Load consumption from the power grid in the commercial area.

Hour	Price (Rs/kWh)	Load consumption from the power grid in commercial area (kW)					
		PSO		COA		mCOA	
		Without RE	With RE	Without RE	With RE	Without RE	With RE
8	12	875	638.06	774.35	537.41	853.5	616.56
9	9.19	1059.4	789.31	976.55	706.46	914.47	644.38
10	12.27	1308.25	1024.41	1205.75	921.91	1018.55	734.71
11	20.69	830.65	532.96	543.65	245.96	692.7	395.01
12	26.82	951.15	649.06	624.15	322.06	583.96	281.87
13	27.35	832.9	551.14	546.4	264.64	556.23	274.47
14	13.81	1387.4	1136.73	1475.9	1225.23	992.5	741.83
15	17.31	1496.3	1281.03	1202.05	986.78	806.95	591.68
16	16.42	1487.9	1318.37	1166.65	997.12	893.25	723.72
17	9.83	1500.15	1379.68	1421.15	1300.68	1162.37	1041.90
18	8.63	1562.7	1451.28	1560.7	1449.28	1298.24	1186.82
19	8.87	1342.45	1230.52	1464.95	1353.02	1266.61	1154.68
20	8.35	1211.45	1105.09	1070.95	964.59	1332.95	1226.59
21	16.44	962.2	864.42	891.2	793.42	820.77	722.99
22	16.19	794.25	699.08	729.5	634.33	841.78	746.61
23	8.87	880.2	789.12	1091.7	1000.62	1315.75	1224.67
24	8.65	921.75	825.73	1033.75	937.73	1380.07	1284.05
1	8.11	1101.7	1001.93	1114.45	1014.68	1312.8	1213.03
2	8.25	1053.95	960.35	1216.7	1123.1	1262.66	1169.06
3	8.1	994.25	901.92	1239.5	1147.17	1335.38	1243.05
4	8.14	833.15	733.83	1068.65	969.33	1256.76	1157.44
5	8.13	758.15	651.15	1134.15	1027.15	1296.78	1189.78
6	8.34	696.9	583.32	1075.65	962.07	1241.63	1128.05
7	9.35	814.3	617.86	1028.05	831.61	1219.84	1023.4

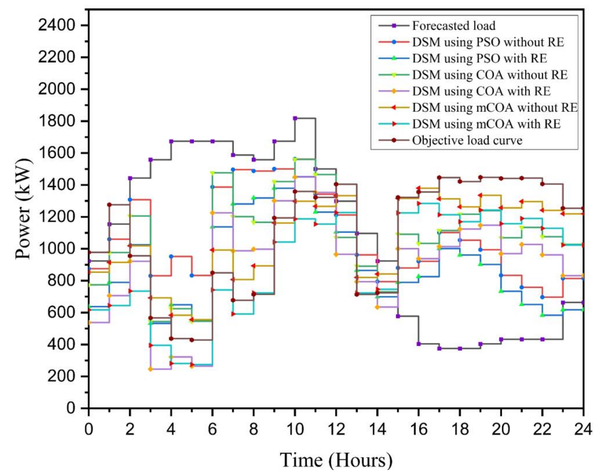

Fig. 4. Load details after applying DSM in the commercial area.

has shown significant improvements in both operational cost savings and peak load reduction. As illustrated in Table 10, the mCOA outperforms both Particle Swarm Optimization (PSO) and the standard Coati Optimization Algorithm (COA) across various scenarios. When renewable energy (RE) sources are excluded, the mCOA achieves a 20.93% reduction in operational costs and a 23.01% decrease in peak load. This remarkable efficiency arises from the algorithm's advanced optimization capabilities, which enable effective load shifting and enhanced load management. The adaptive features of the mCOA help mitigate peak demand by strategically redistributing loads to off-peak periods. The reduced Peak-to-Average Ratio (PAR) further demonstrates the algorithm's success in creating a balanced load profile. With the incorporation of RE sources, the mCOA's advantages become even clearer, resulting in a 28.25% drop in operational costs and a 26.64% decrease in peak load. These improvements can be attributed to the mCOA's ability to optimally utilize renewable energy, thereby decreasing its reliance on traditional energy sources. By efficiently integrating RE generation, the algorithm not only lowers energy costs but also promotes the sustainability of the industrial grid. Compared to PSO and COA, the mCOA consistently achieves superior results in terms of cost savings and peak load reduction.

Additionally, the performance of the mCOA algorithm is

Table 10. Cost of energy and peak load of the industrial smart grid after the application of DSM.

Optimization technique	Peak load (kW)		PAR		Cost (Rupees)	
	Peak load	% reduction	PAR	% reduction	Cost	% reduction in cost
without DSM	2727.3	-	1.617	-	571204.7	-
[28] without RE	2335.1	14.38	1.384	14.38	463761.1	18.81
PSO without RE	2181.1	20.02	1.293	20.03	461717.8	19.16
COA without RE	2126.64	22.02	1.261	22.01	442395.4	22.55
mCOA without RE	2099.88	23.01	1.245	23.01	451641.9	20.93
[28] with RE	2315.1	15.11	1.372	15.11	453536.5	20.60
PSO with RE	1979.8	27.40	1.289	20.65	419886.3	26.49
COA with RE	2015.22	26.10	1.319	18.42	400563.9	29.87
mCOA with RE	2000.62	26.64	1.314	18.73	409810.4	28.25
PSO with RE and battery	1965.88	27.91	1.281	20.77	420099.3	26.45
COA with RE and battery	1985.22	27.20	1.301	19.54	400777.0	29.83
mCOA with RE and battery	2028.04	25.63	1.332	17.62	410023.5	28.21

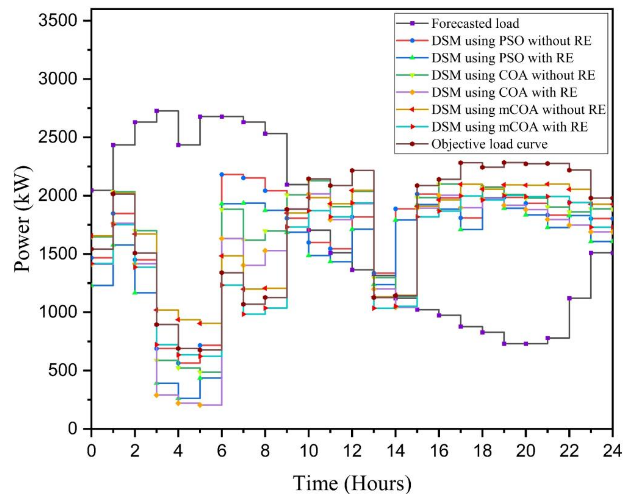

Fig. 5. Load details after applying DSM in industrial area.

evaluated with integrated battery storage. With this integration, the algorithm consistently shows strong results, achieving a 28.21% cost reduction and a 25.63% decrease in peak load. The efficient management of energy storage by the algorithm enhances load flexibility, allowing for reduced reliance on the grid during peak periods. This advantage is especially relevant in industrial settings, where energy demands often fluctuate. The hourly load consumption data, shown in Table 11, further validates the effectiveness of the mCOA. The algorithm consistently demonstrates lower energy consumption than PSO and COA, particularly during periods of high prices. By shifting non-essential loads to off-peak times, the mCOA effectively lowers operational costs while ensuring reliable grid operations. Moreover, the algorithm's precise adherence to the targeted load curve, depicted in Fig. 5, underscores its accuracy in load prediction and management. Compared to alternative algorithms, the mCOA is distinguished by its adaptive exploration-exploitation mechanism, which mitigates premature convergence and promotes optimal decision-making. This feature is particularly beneficial for industrial applications, where maintaining efficiency and cost-effectiveness is vital. In summary, the mCOA's capacity to deliver significant cost savings and peak load reductions positions it as a reliable and effective optimization solution for industrial demand-side management.

Table 11. Load consumption from the power grid in the industrial area.

Hour	Price (Rs/kWh)	Load consumption from the power grid in industrial area (kW)					
		PSO		COA		mCOA	
		Without RE	With RE	Without RE	With RE	Without RE	With RE
8	12	1466.75	1229.81	1647.45	1410.51	1654.87	1417.93
9	9.19	1847.35	1577.26	2033.4	1763.31	2021.57	1751.48
10	12.27	1450.65	1166.81	1700.25	1416.41	1670.57	1386.73
11	20.69	688.8	391.11	586.94	289.25	1020.07	722.38
12	26.82	564.1	262.01	522.57	220.48	936.51	634.42
13	27.35	716.6	434.84	486.4	204.64	903.88	622.12
14	13.81	2181.1	1930.43	1882.3	1631.63	1482.76	1232.09
15	17.31	2151.15	1935.88	1618.4	1403.13	1198.23	982.96
16	16.42	2042.5	1872.97	1697.15	1527.62	1205.77	1036.24
17	9.83	1806.45	1685.98	2006.75	1886.28	1851.4	1730.93
18	8.63	1598	1486.58	2126.64	2015.22	1983.05	1871.63
19	8.87	1545.7	1433.77	1905.35	1793.42	1930.21	1818.28
20	8.35	1817.35	1710.99	2037.45	1931.09	2044.1	1937.74
21	16.44	1335.4	1237.62	1296.85	1199.07	1132.76	1034.98
22	16.19	1886.35	1791.18	1137.15	1041.98	1146.14	1050.97
23	8.87	2013.95	1922.87	1983.53	1892.45	1909.35	1818.27
24	8.65	1980.75	1884.73	2098.95	2002.93	1963.09	1867.07
1	8.11	1808.85	1709.08	1996.23	1896.46	2097.81	1998.04
2	8.25	2073.4	1979.8	2069.58	1975.98	2056.04	1962.44
3	8.1	1984	1891.67	2009.4	1917.07	2092.95	2000.62
4	8.14	1933.75	1834.43	1979.5	1880.18	2089.62	1990.30
5	8.13	1833.2	1726.2	1902.75	1795.75	2099.88	1992.88
6	8.34	1941.6	1828.02	1860.2	1746.62	2053.75	1940.17
7	9.35	1802.95	1606.51	1885.51	1689.07	1926.32	1729.88

The application of load shifting-based DSM in SG has been simulated using the LabVIEW-2022 software application with the help of a personal computer with an AMD Ryzen 5 processor equipped with sixteen gigabytes of memory. The convergence graphs obtained after applying PSO, COA, and mCOA in residential, commercial, and industrial areas are represented in Figs. 6, 7, and 8, respectively. The convergence graphs show that the proposed mCOA algorithm converges faster when compared with PSO and COA algorithms.

Quantifying the degree of variation or dispersion in a data set is done statistically using the standard deviation. For several reasons, Standard Deviation (SD) can be important when evaluating optimization approaches. While implementing an optimization algorithm, the outcome varies for individual run. So, to assess an optimization technique, the program must be run several times, and the SD must be found to determine the deviation of the outcome from a standard value. This article used simulation studies for the PSO, COA, and mCOA-based DSM implementation in a smart grid to reduce the cost and peak load. These simulations were carried out for 50 independent runs and found SD in residential, commercial, and industrial areas for cost and peak load, as shown in Table 12. From the table it has been noted that the performance of mCOA is better than other optimizations.

4.4. Emission analysis

Total emissions generated in the system are calculated by assuming the constant emission generated per kW. When the system has some renewable energy sources, the total emissions will be reduced since the power drawn from the grid will be reduced even though there are no emissions released from renewable energy generation, emissions released while manufacturing, maintaining, and disposing of the renewable energy generators which are included in life cycle analysis. A life cycle analysis (LCA) evaluates the total emissions linked to a product, process, or service throughout its entire life cycle, from "cradle to grave." This includes assessing emissions at every stage, such as raw material extraction, production, transportation, usage, and disposal. LCA provides insight into the full environmental impact of various technologies and products by considering both direct and indirect emissions. For solar PV panels, about 42 grams of CO_2 is produced per kWh of energy for the first 3 years, and then it is said to be almost carbon neutral. About 60% to 70% of emissions released only during manufacturing consist of raw material extraction, material production, module manufacturing, system component manufacturing, and plant installation. 20% to 25% of emissions were released during the operation, involving power generation,

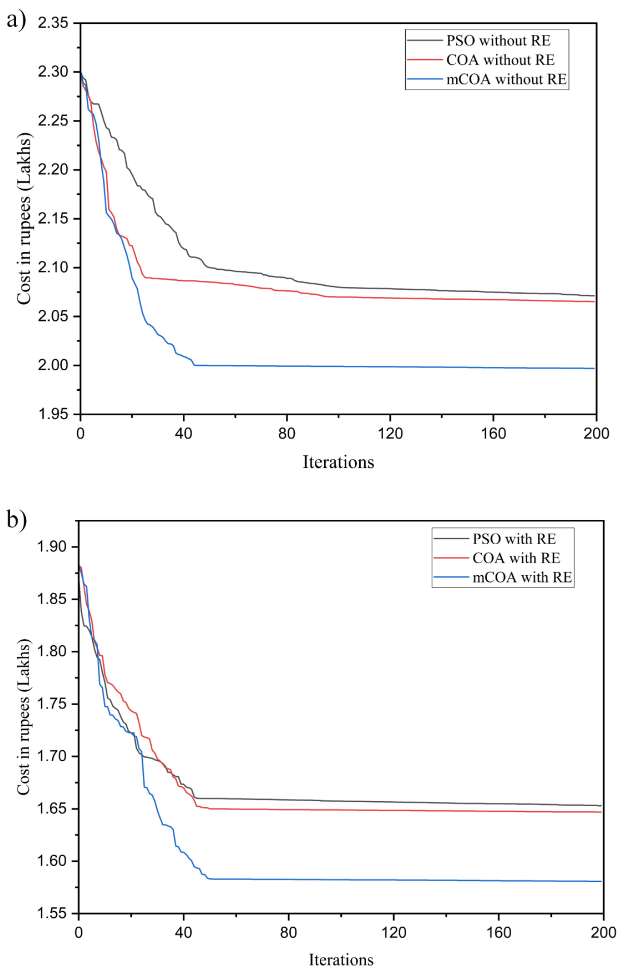

Fig. 6. Convergence graph of PSO, COA, and mCOA performance with the application of DSM in the residential area. (a) Without the presence of RE sources. (b) With the presence of RE sources.

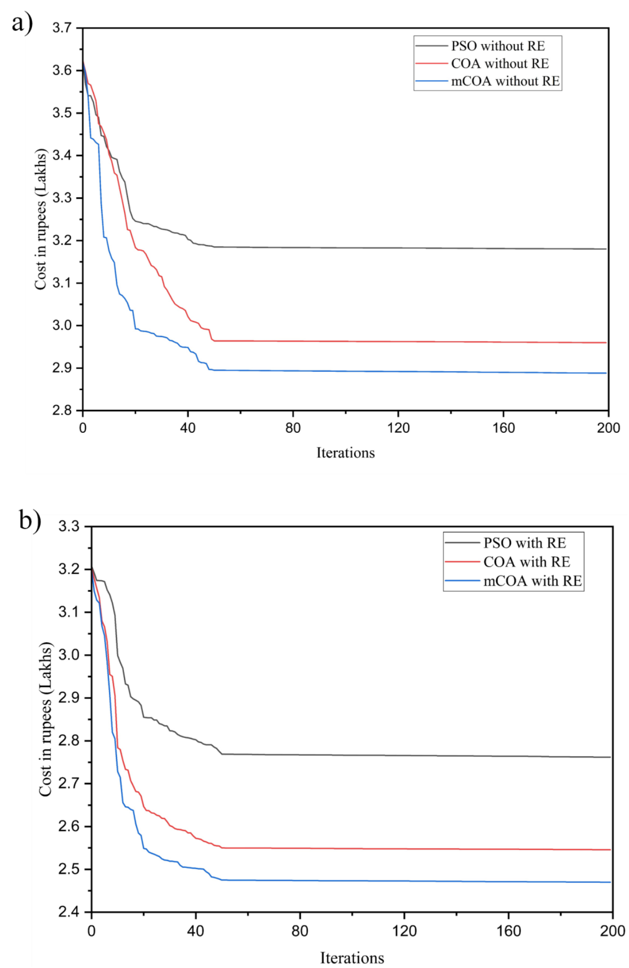

Fig. 7. Convergence graph of PSO, COA, and mCOA performance with the application of DSM in a commercial area. (a) Without the presence of RE sources. (b) With the presence of RE sources.

system operation, and maintenance. The remaining emissions were released when the plant was decommissioned.

With the help of Eq. (16), the total emission generated can be calculated. With the help of existing renewable energy generation, there is a reduction of 3788.73 kg of emissions in each area, and these can be further classified as a reduction in CO_2, SO_2, and NO as 3743.11 kg, 28.37 kg, and 17.25 kg, respectively. With the help of pictorial representation, the difference in emissions with and without RE is shown in Fig. 9.

4.5. Limitations of the proposed model

The key limitations of the proposed model are as follows:

- **Algorithm performance on specific cases:** While the Modified Coati Optimization Algorithm (mCOA) showed superior performance in DSM implementation, achieving faster convergence and notable cost savings, it fell short compared to other algorithms in certain specific benchmark functions (Tables 4 and 5).
- **Premature convergence in industrial load areas:** The proposed DSM architecture, tested across residential, commercial, and industrial sectors, showed reliable convergence. However, the algorithm occasionally experienced premature convergence in the industrial sector, similar to other optimization algorithms, leading to performance comparable to existing methods.
- **Renewable energy uncertainty:** The model does not incorporate advanced forecasting techniques for renewable energy variability, which may impact system reliability under high penetration levels.
- **Scalability issues:** While the model performs efficiently for medium-scale systems, computational complexity may increase with large-scale implementations, affecting execution time.
- **Hardware and implementation constraints:** Practical deployment depends on the availability of smart grid infrastructure and real-time demand-side management technologies.

The load scheduling DSM technique is successfully implemented in all three load zones, resulting in a considerable decrease in utility costs and peak load. With more controllable devices, the distribution grid's performance may be enhanced. However, the addition of controlled devices will also increase complexity. Both the utility and the customers may save more money with smart scheduling. The comfort level of clients affects the cost savings and peak load. With the protracted delays encountered by the customers while the operator shifts the loads, consumer satisfaction levels must be considered. The DSM will produce subpar results since it is difficult to attain a valley point quickly with fewer time delays. Integrating renewable energy resources such as wind and solar will provide more provisions to reduce the cost and peak load in the system. With the help of RE, the reduction in the cost of electricity is more significant than the system operated with DSM alone.

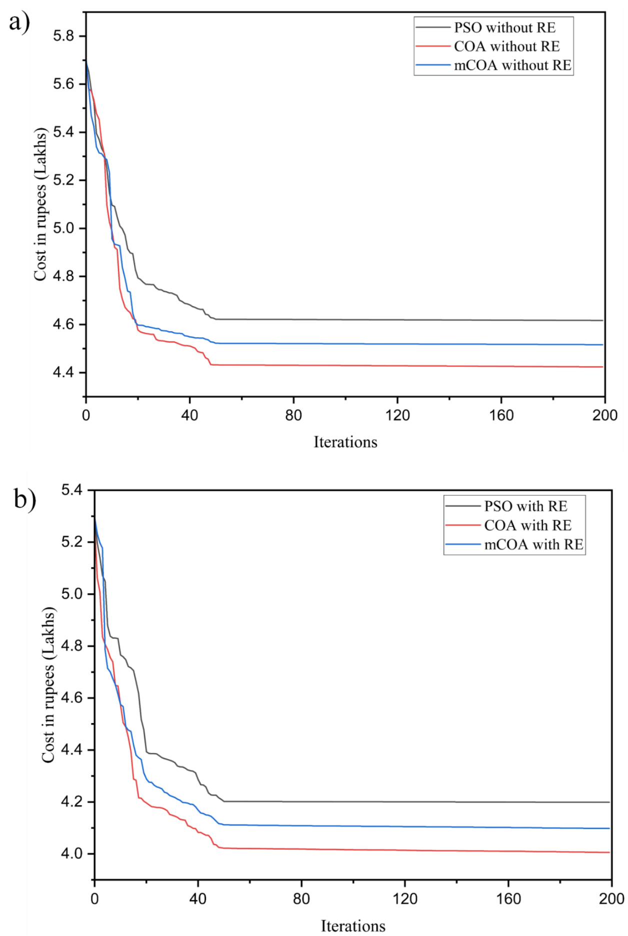

Fig. 8. Convergence graph of PSO, COA, and mCOA performance with the application of DSM in industrial area. (a) Without the presence of RE sources. (b) With the presence of RE sources.

Table 12. Standard Deviation (SD) of PSO, COA, and mCOA.

DSM area	SD of PSO		SD of COA		SD of mCOA	
	Cost (Rupees)	Peak load (kW)	Cost (Rupees)	Peak load (kW)	Cost (Rupees)	Peak load (kW)
Residential	2123.40	19.21	2095.13	18.91	2040.34	18.85
Commercial	5242.24	31.65	5120.26	30.96	5041.23	28.96
Industrial	7013.65	46.56	6945.62	48.23	6972.36	47.485

5. Conclusion

This study presents a comprehensive demand-side management (DSM) strategy for a smart distribution system that encompasses various load sectors, comprising both controllable and uncontrollable loads. The objective is to reduce peak demand, lower energy costs, and minimize emissions by employing a day-ahead load scheduling method within a life cycle analysis (LCA) framework. The integration of hybrid renewable energy sources (RE) and a battery energy storage system (BESS) significantly enhances the system's flexibility and sustainability, effectively addressing the intermittent nature of renewables. The optimized DSM strategy employs a novel modified Coati Optimization Algorithm (mCOA), showcasing significant improvements over traditional algorithms, including Particle Swarm Optimization (PSO) and the standard Coati Optimization Algorithm (COA). For the residential, commercial, and industrial sectors, the mCOA yielded significant cost savings and reductions in peak load. In the commercial sector, for example, it achieved a 20.35% decrease in energy expenses and a 24.09% reduction in peak load without

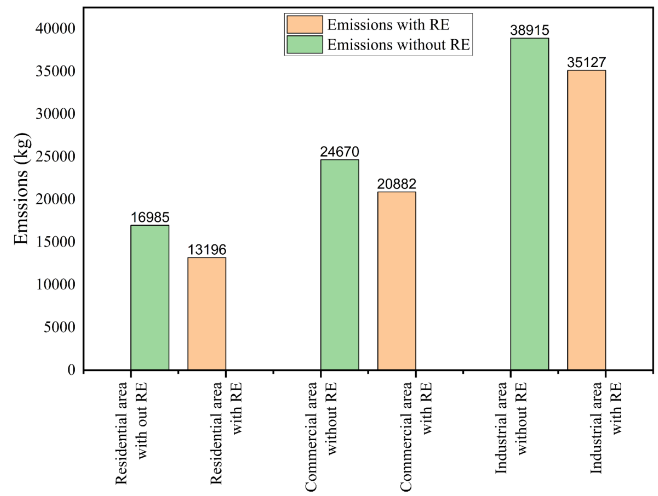

Fig. 9. Total emissions in residential, industrial, and commercial areas.

RE integration, with further enhancements of 31.89% in savings and 29.37% in peak load reduction with RE. Similarly, in the industrial sector, the mCOA achieved up to 28.25% in cost savings and a 26.64% decrease in peak load with the integration of RE. The study also emphasized the role of BESS in enhancing system performance. With battery storage, the mCOA effectively reduced energy costs and peak demand by shifting loads and storing excess renewable energy. Consequently, the commercial and industrial sectors experienced cost reductions of 31.83% and 28.21%, along with peak load reductions of 27.72% and 25.63%. Furthermore, the LCA provided practical insights into emissions from renewable energy sources, offering a more accurate estimate of environmental impacts compared to conventional methods that often overlook emissions associated with RE production and operation. By assessing the real-time effects of integrating renewable energy, the study delivered a more thorough evaluation of the DSM strategy. The resulting load curves validated the mCOA's efficiency in maintaining a stable load profile while reducing costs and peak demand. The algorithm excelled in adapting to load variations and ensuring optimal load distribution, outperforming PSO and COA in tracking the target load curve, thereby confirming its robustness and efficiency. In summary, the mCOA-based DSM strategy presents a reliable and effective method for managing smart distribution grids. It skillfully addresses the multi-constrained DSM challenge by balancing load demands, optimizing energy usage, and promoting sustainability through the integration of RE and BESS. This study establishes a scalable and flexible framework for future smart grid developments, contributing to sustainable energy management and reduced carbon emissions.

Declarations

Competing interests: The authors did not receive financial and non-financial support from any organization for the submitted work. The authors have no competing interests to declare that are relevant to the content of this article.

Data availability: The authors declare that the data supporting the findings of this study are available within this research article.

Author contributions: Conceptualization: [Sampatirao Nanibabu]; Methodology: [Sampatirao Nanibabu]; Formal analysis and investigation: [Sampatirao Nanibabu], [Shakila Baskaran]; Writing - original draft preparation: [Sampatirao Nanibabu]; Writing - review and editing: [Shakila Baskaran], [Prakash Marimuthu]; Resources: [Prakash Marimuthu]; Supervision: [Shakila Baskaran].

References

[1] G. Dileep, “A survey on smart grid technologies and applications,” *Renewable Energy*, vol. 146, pp. 2589–2625, 2020.

[2] X. Gao, Y. Zhang, F. Ji, and L. Fu, “A demand side management strategy to reduce the impact of high power pulse load integration,” *J. Electr. Eng. Technol.*, vol. 17, no. 5, pp. 2663–2674, 2022.

[3] T. Nasir, S. S. H. Bukhari, S. Raza, H. M. Munir, M. Abrar, H. A. U. Muqeet, and R. Masroor, “Recent challenges and methodologies in smart grid demand side management: State-of-the-art literature review,” *Math. Probl. Eng.*, vol. 2021, pp. 1–16, 2021.

[4] A. Sardar, S. U. Khan, M. A. Hassan, *et al.*, “A demand side management scheme for optimal power scheduling of industrial loads,” *Energy Syst.*, vol. 14, pp. 335–356, 2023.

[5] H. Golmohamadi, “Demand-side management in industrial sector: A review of heavy industries,” *Renew. Sustain. Energy Rev.*, vol. 156, p. 111963, 2022.

[6] R. Dharani, M. Balasubramonian, T. S. Babu, and B. Nastasi, “Load shifting and peak clipping for reducing energy consumption in an indian university campus,” *Energies*, vol. 14, no. 3, p. 558, 2021.

[7] D. Kanakadhurga and N. Prabaharan, “Demand side management in microgrid: A critical review of key issues and recent trends,” *Renew. Sustain. Energy Rev.*, vol. 156, p. 111915, 2022.

[8] A. K. Sharma and A. Saxena, “A demand side management control strategy using whale optimization algorithm,” *SN Appl. Sci.*, vol. 1, no. 8, p. 870, 2019.

[9] G. R. Goyal and S. Vadhera, “Solution to objectives of supply side energy management by integrating enhanced demand response strategy,” *J. Oper. Autom. Power Eng.*, vol. 12, no. 4, pp. 269–279, 2024.

[10] D. Mariano-Hernández, L. Hernández-Callejo, A. Zorita-Lamadrid, O. Duque-Pérez, and F. S. García, “A review of strategies for building energy management system: Model predictive control, demand side management, optimization, and fault detect & diagnosis,” *J. Build. Eng.*, vol. 33, p. 101692, 2021.

[11] R. S. Kumar, L. P. Raghav, D. K. Raju, and A. R. Singh, “Intelligent demand side management for optimal energy scheduling of grid connected microgrids,” *Appl. Energy*, vol. 285, p. 116435, 2021.

[12] F. Jabari, M. Nazari-Heris, and M. Abapour, “Implementation and investigation of demand-side management polices in iran’s industrial and commercial sectors,” *J. Energy Manag. Technol.*, vol. 7, no. 1, pp. 34–42, 2023.

[13] D. S. S. Mohammed, M. M. Othman, O. O. Mohammed, M. Ahmadipour, and M. L. Othman, “Saving utility costs optimization in generator operation planning based on scalable alternatives of probabilistic demand-side management,” *Sustain. Energy Technol. Assess.*, vol. 75, p. 104258, 2025.

[14] R. B. Navesi, A. F. Naghibi, H. Zafarani, H. Tahami, and S. Pirouzi, “Reliable operation of reconfigurable smart distribution network with real-time pricing-based demand response,” *Electr. Power Syst. Res.*, vol. 241, p. 111341, 2025.

[15] M. Ramesh and R. P. Saini, “Demand side management based techno-economic performance analysis for a stand-alone hybrid renewable energy system of india,” *Energy Sources A: Recovery, Util. Environ. Eff.*, vol. 47, no. 1, pp. 3359–3387, 2025.

[16] H. Jouma, M. Mansor, M. S. Abd Rahman, Y. Jia Ying, and H. Mokhlis, “Influence of the demand side management on the daily performance of microgrids in smart environments using grey wolf optimizer,” *Smart Sustain. Built Environ.*, 2024.

[17] A. Rollo, P. Serafini, F. Aleotti, D. Cilio, E. Morandini, D. Moneta, and V. Angelucci, “Load shifting and demand-side management in renewable energy communities: Simulations of different technological configurations,” *Energies*, vol. 18, no. 4, p. 872, 2025.

[18] S. Nanibabu, S. Baskaran, and P. Marimuthu, “Realisation of demand side management in smart distribution grid with commercial loads using butterfly optimization algorithm,” in *2024 Third Int. Conf. Intell. Techniq. Control, Optim. Signal Proc.*, pp. 1–6, IEEE, 2024.

[19] B. N. Alhasnawi, B. H. Jasim, A. N. Alhasnawi, F. F. K. Hussain, R. Z. Homod, H. A. Hasan, and B. E. Sedhom, “A novel efficient energy optimization in smart urban buildings based on optimal demand side management,” *Energy Strat. Rev.*, vol. 54, p. 101461, 2024.

[20] M. Ahang, P. M. S. Seljom, and A. Tomasgard, “Analysis of the impact of demand response on the norwegian energy system,” *Energy Syst.*, 2023.

[21] M. Al-Dhaifallah, Z. Alaas, A. Rezvani, B. N. Le, and S. Samad, “Optimal day-ahead economic/emission scheduling of renewable energy resources based microgrid considering demand side management,” *J. Build. Eng.*, vol. 76, p. 107070, 2023.

[22] Y. Yang, S. Bremner, C. Menictas, and M. Kay, “Battery energy storage system size determination in renewable energy systems: A review,” *Renew. Sustain. Energy Rev.*, vol. 91, pp. 109–125, 2018.

[23] S. K. Jha and D. Kumar, “Demand side management for stand-alone microgrid using coordinated control of battery energy storage system and hybrid renewable energy sources,” *Electr. Power Compon. Syst.*, vol. 47, no. 14-15, pp. 1261–1273, 2019.

[24] C. Cruz, M. Tostado-Véliz, E. Palomar, and I. Bravo, “Pattern-driven behaviour for demand-side management: An analysis of appliance use,” *Energy Build.*, vol. 308, p. 113988, 2024.

[25] R. Khezri, A. Mahmoudi, and M. H. Haque, “A demand side management approach for optimal sizing of standalone renewable-battery systems,” *IEEE Trans. Sustain. Energy*, vol. 12, no. 4, pp. 2184–2194, 2021.

[26] K. Ullah, T. A. Khan, G. Hafeez, I. Khan, S. Murawwat, B. Alamri, and S. Khan, “Demand side management strategy for multi-objective day-ahead scheduling considering wind energy in smart grid,” *Energies*, vol. 15, no. 19, p. 6900, 2022.

[27] N. Javaid, G. Hafeez, S. Iqbal, N. Alrajeh, M. S. Alabed, and M. Guizani, “Energy efficient integration of renewable energy sources in the smart grid for demand side management,” *IEEE Access*, vol. 6, pp. 77077–77096, 2018.

[28] R. K. Yadav, P. N. Hrisheekesha, and V. S. Bhadoria, “Grey wolf optimization-based demand side management in solar pv integrated smart grid environment,” *IEEE Access*, vol. 11, pp. 11827–11839, 2023.

[29] D. K. Geleta, M. S. Manshahia, P. Vasant, and A. Banik, “Grey wolf optimizer for optimal sizing of hybrid wind and solar renewable energy system,” *Comput. Intell.*, vol. 38, no. 3, pp. 1133–1162, 2022.

[30] B. N. Silva, M. Khan, R. E. Wijesinghe, and U. Wijenayake, “Meta-heuristic optimization based cost efficient demand-side management for sustainable smart communities,” *Energy Build.*, vol. 303, p. 113599, 2024.

[31] A. A. Almehizia, H. M. Al-Masri, and M. Ehsani, “Integration of renewable energy sources by load shifting and utilizing value storage,” *IEEE Trans. Smart Grid*, vol. 10, no. 5, pp. 4974–4984, 2018.

[32] S. Ali, K. Ullah, G. Hafeez, I. Khan, F. R. Albogamy, and S. I. Haider, “Solving day-ahead scheduling problem with multi-objective energy optimization for demand side

management in smart grid," *Eng. Sci. Technol. Int. J.*, vol. 36, p. 101135, 2022.

[33] T. Logenthiran, D. Srinivasan, and T. Z. Shun, "Demand side management in smart grid using heuristic optimization," *IEEE Trans. Smart Grid*, vol. 3, no. 3, pp. 1244–1252, 2012.

[34] S. Zhou, H. He, L. Zhang, W. Zhao, and F. Wang, "A data-driven method to monitor carbon dioxide emissions of coal-fired power plants," *Energies*, vol. 16, no. 4, p. 1646, 2023.

[35] H. O. Omotoso, A. M. Al-Shaalan, H. M. Farh, and A. A. Al-Shamma'a, "Techno-economic evaluation of hybrid energy systems using artificial ecosystem-based optimization with demand side management," *Electron.*, vol. 11, no. 2, p. 204, 2022.

[36] F. A. B. Zaini, M. F. Sulaima, I. A. W. A. Razak, N. I. Zulkafli, and H. Mokhlis, "A review of pso-based algorithm application in demand side management: Challenges & opportunities," *IEEE Access*, 2023.

[37] M. Dehghani, Z. Montazeri, E. Trojovská, and P. Trojovský, "Coati optimization algorithm: A new bio-inspired metaheuristic algorithm for solving optimization problems," *Knowledge-Based Syst.*, vol. 259, p. 110011, 2023.

[38] S. Arora and S. Singh, "Butterfly optimization algorithm: a novel approach for global optimization," *Soft Comput.*, vol. 23, pp. 715–734, 2019.